On the stability of a cylindrical liquid bridge

Vlado A. Lubarda

Acta Mechanica

ISSN 0001-5970
Volume 226
Number 2

Acta Mech (2015) 226:233-247
DOI 10.1007/s00707-014-1158-5

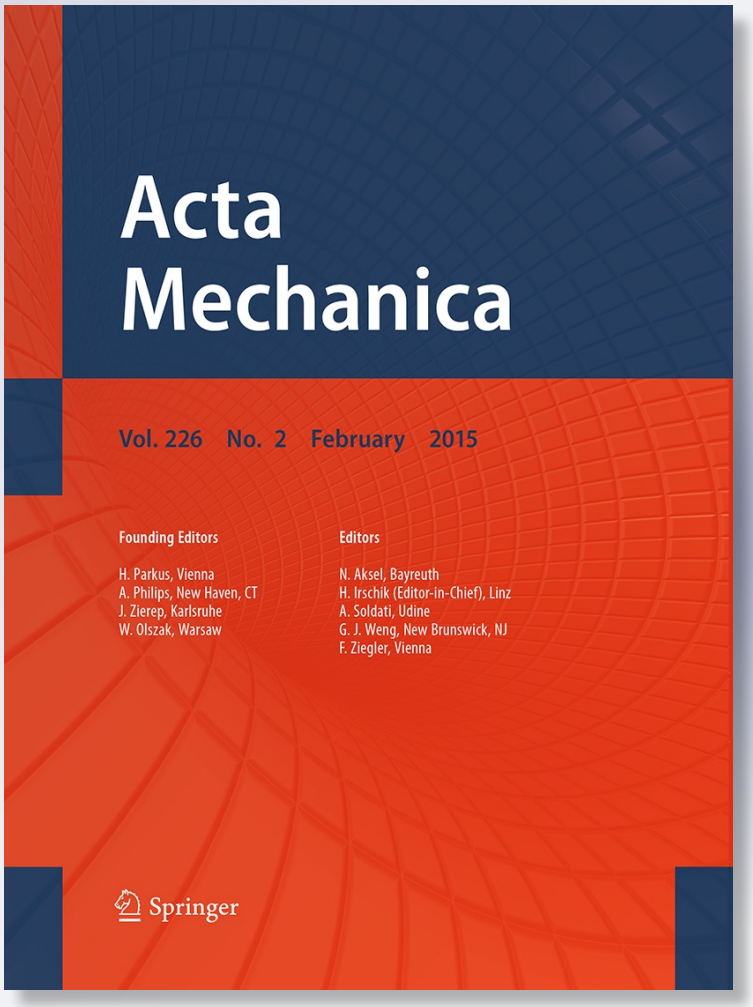

Springer

Acta Mech 226:233–247 (2015)
DOI 10.1007/s00707-014-1158-5

Vlado A. Lubarda

On the stability of a cylindrical liquid bridge

Received: 9 January 2014 / Revised: 3 April 2014 / Published online: 13 June 2014

Abstract The problem of the stability of a liquid bridge stretched between parallel plates with a wetting contact angle of 90° is revisited. A closed form expression is derived for the height of the bridge, in terms of its volume, within which a cylindrical and various types of unduloidal equilibrium configurations can exist. For a given volume of the liquid and specified height of the bridge, the lateral surface of a uniform cylindrical bridge is smaller than the surface area of any unduloidal equilibrium shape. The lateral surface of the unduloidal shapes increases with the increase in the number of their inflection points. The force required to keep the bridge in equilibrium is evaluated in each case. All unduloidal equilibrium configurations are unstable, the only stable configuration being that of a cylindrical bridge whose height is less than one-half of its circumference. A lower bound estimate is also derived based on a simple energy consideration. The stretching force required for the equilibrium at the onset of instability is compared with its upper bound estimate. For a given height of the bridge, the force required to keep a cylindrical bridge in equilibrium is greater than the force required for equilibrium of any unduloidal configuration of the same height. The opposite is true for the capillary pressure.

1 Introduction

Liquid bridges form in many cases of technological importance, which include tribological problems, coating, metallic melts and crystal growth, mechanics of porous media, powder technology, cree rapture, and various problems of bio- and nanomechanics. For example, a liquid bridge can form from a liquid condensate at the interface between two spherical particles, between a spherical particle and a flat substrate, between a solid body and a liquid surface, between grain boundaries, between crack faces, and between the tip of an atomic force microscope and a substrate. Consequently, considerable amount of research was devoted to analytical and experimental determination of the capillary binding forces due to liquid bridges at the solid/solid or solid/liquid interfaces, e.g., [1–3]. The stability of liquid bridges between coaxial parallel disks, with or without gravity effects, for which the contact angle between liquid and disks may vary freely within the interval specified by the contact angles with the two sides of each disk (canthotaxis effect). In the stability analysis of liquid bridges between parallel plates, on the other hand, the contact angle between liquid and supporting plates is fixed (Neumann-type boundary condition), but the contact boundary can vary. This has been studied in great detail for arbitrary, either equal or different contact angles, by many researchers [4–13]. The critical height of the cylindrical bridge, with the contact angle of 90°, was first established by Vogel [4] and Athanassenas [5],

V. A. Lubarda (✉)
Department of Nano-Engineering and Mechanical and Aerospace Engineering,
University of California, San Diego, La Jolla, CA 92093-0448, USA
E-mail: vlubarda@ucsd.edu

V. A. Lubarda
Montenegrin Academy of Sciences and Arts, Rista Stijovića 5, 81000 Podgorica, Montenegro

who also proved that all unduloidal bridge configurations with 90° contact angle are unstable. Liquid bridges between balls, liquid ridges, doubly connected liquid surfaces in cylindrical containers, and the rotating liquid bridges which can develop an amphora or a skipping rope instability have also been studied; the representative references include [14–20]. The effect of the axial acceleration or the axial magnetic field on the stability of the bridge have been examined in [21,22]. For a related topic of the equilibrium and stability of sessile and pendant drops, the references [23–27] can be consulted.

The objective of this paper is to provide a physically motivated, conceptually simple analysis of the onset of instability of a cylindrical liquid bridge between two parallel flat plates, as the bridge is slowly stretched by pulling the plates apart. This instability onset was originally established by variational analysis from a rigorous mathematical point of view by Vogel [4] and Athanassenas [5]. The expressions are derived for the heights of the bridge within which either cylindrical or various unduloidal equilibrium configurations represent possible equilibrium configurations. It is shown that, for a given volume of the liquid and specified height of the bridge, the lateral surface of a uniform cylindrical bridge is smaller than the surface area of any unduloidal equilibrium configuration. A simple proof is constructed to show that all unduloidal equilibrium bridge configurations are unstable and that the only stable equilibrium configuration is that of a cylindrical bridge whose height is less than one-half of its circumference [4,5]. A lower bound estimate of the critical aspect ratio is then derived based on a simple energy consideration. The stretching force required to keep the bridge in equilibrium at the onset of instability is compared with its upper bound estimate.

2 Cylindrical liquid bridge

Figure 1a shows the equilibrium configuration of a liquid drop resting on a solid substrate (plate) with the wetting contact angle of 90°. If the liquid volume is V, a drop whose bounding surface has the least surface energy is a hemispherical drop of radius $R_1 = (3V/2\pi)^{1/3}$, provided that the gravity (g) is absent or that its effect on the flattening of the drop can be neglected. The latter assumption is acceptable provided that the size of the drop is less than the capillary length $(\sigma/\rho g)^{1/2}$, where ρ is the density of the liquid, and σ is the liquid/vapor surface (interface) energy [28].

If another plate approaches the drop from above, parallel to the lower plate (Fig. 1b), upon its contact with the drop, the drop looses its equilibrium with any further approach of the plates. The adhesive forces between the plates and liquid set in and pull the plates toward each other, while the liquid spreads outward forming a liquid bridge. If the separation between wetted plates is $H < R_1$, the only possible equilibrium configuration is a cylindrical bridge whose base radius is $R = (V/\pi H)^{1/2}$ (as elaborated in Sect. 3), provided that a pair of resistive forces F is supplied externally to balance the capillary attraction and the Laplace pressure (Fig. 2). The magnitude of this force is

$$F = 2R\pi\sigma - R^2\pi\Delta p = R\pi\sigma, \tag{1}$$

where $\Delta p = 2\sigma\kappa = \sigma/R$ is the Laplace pressure, and $\kappa = (2R)^{-1}$ is the mean curvature of the lateral surface of the bridge. It is noted that in the case of 90° contact angle, there is no surface energy interchange caused by the wetting of the plates, because the solid/liquid and solid/vapor interface energies are equal to each other ($\sigma_{sl} = \sigma_{sv} = \sigma$).

Suppose now that the bridge is quasi-statically stretched by slowly pulling the plates apart, under the displacement controlled conditions. Following the transient liquid flow associated with each increment of

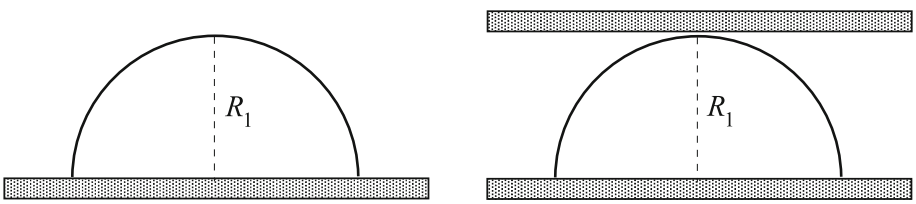

Fig. 1 **a** A hemispherical liquid drop resting on a flat plate. Its radius is $R_1 = (3V/2\pi)^{1/3}$, where V is the liquid volume. **b** Another plate approaching the drop, just before being pushed into the drop

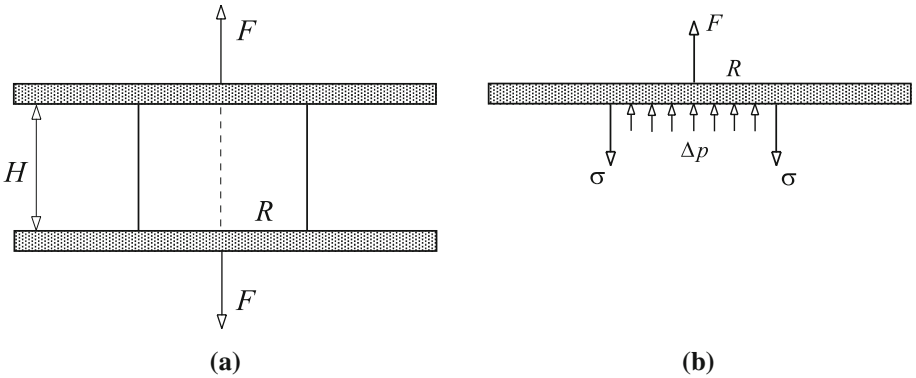

Fig. 2 **a** A cylindrical liquid bridge of radius R and height H between two parallel plates. **b** The capillary forces and the Laplace pressure exerted by the liquid on the plates are equilibrated by the externally applied forces F

stretch,[1] the magnitude of the applied force is decreased, as needed for the new equilibrium configuration. The question is at what value of the force F, and at what aspect ratio H/R, the cylindrical bridge looses its stability. In particular, we want to address this question in light of the fact that a nonlinear differential equation for the liquid shape $2\sigma\kappa = \Delta p$ may have multiple solutions. Indeed if the separation of the plates is $H = H_1 = (3V/2\pi)^{1/3}$, either a hemispherical or cylindrical shape can fit between the plates (both being surfaces of constant curvature). The separation of the plates spanned by $n \geq 1$ adjacent hemispherical surface segments is[2]

$$H_n = n^{2/3}\, H_1, \quad H_1 = \left(\frac{3V}{2\pi}\right)^{1/3}, \tag{2}$$

which is obtained from the conditions

$$H_n = n R_n, \quad V = \frac{2n}{3}\, R_n^3 \pi. \tag{3}$$

The configurations for $n = 1,\ 2,\ 3$, and 4 are shown in Fig. 3. The corresponding lateral surface is $S_n = 2n R_n^2 \pi$, or, in terms of the liquid volume,

$$S_n = 2\pi n^{1/3}\, H_1^2. \tag{4}$$

The radius ρ_n of the cylindrical bridge of height H_n, occupying the same volume V, is obtained from $\rho_n^2 \pi H_n = V$. This gives

$$\rho_n = \sqrt{\frac{2}{3}}\, \frac{H_1}{n^{1/3}}. \tag{5}$$

The lateral surface of this cylinder is $s_n = 2\pi\rho_n H_n$ so that

$$s_n = \sqrt{\frac{2}{3}}\, S_n < S_n. \tag{6}$$

The aspect ratio of the cylinder is $H_n/\rho_n = \sqrt{3/2}\, n$. The force required for the equilibrium of such a cylindrical bridge is

$$\hat{F}_n = \rho_n \pi \sigma = \left(\frac{2}{3}\right)^{1/6} \left(\frac{\pi^2 V}{n}\right)^{1/3} \sigma = \left(\frac{2}{3}\right)^{1/2} \frac{\pi H_1}{n^{1/3}}\, \sigma. \tag{7}$$

The sequence of the increasing heights (the plate separations) $\{H_n\}$, scaled by $H_1 = (3V/2\pi)^{1/3}$, is

$$\frac{\{H_n\}}{H_1} = \{n^{2/3}\} = \{1,\ 1.587,\ 2.08,\ 2.52,\ 2.924,\ 3.302,\ 3.659,\ 4,\ 4.327,\ 4.642,\ \ldots\}. \tag{8}$$

[1] The initial increase of the force applied during each incremental stretch supplies inertial effects for the transient fluid flow, which are damped out by the viscosity of the fluid in reaching the equilibrium configuration.

[2] The unduloidal surface consists of the sequence of attached spheres in the limit as $\varphi_* \to \pi/2$ (see Sect. 3). In this case $c = 0$ and (10) gives $r/\cos\varphi = \kappa^{-1}$ = radius of the sphere.

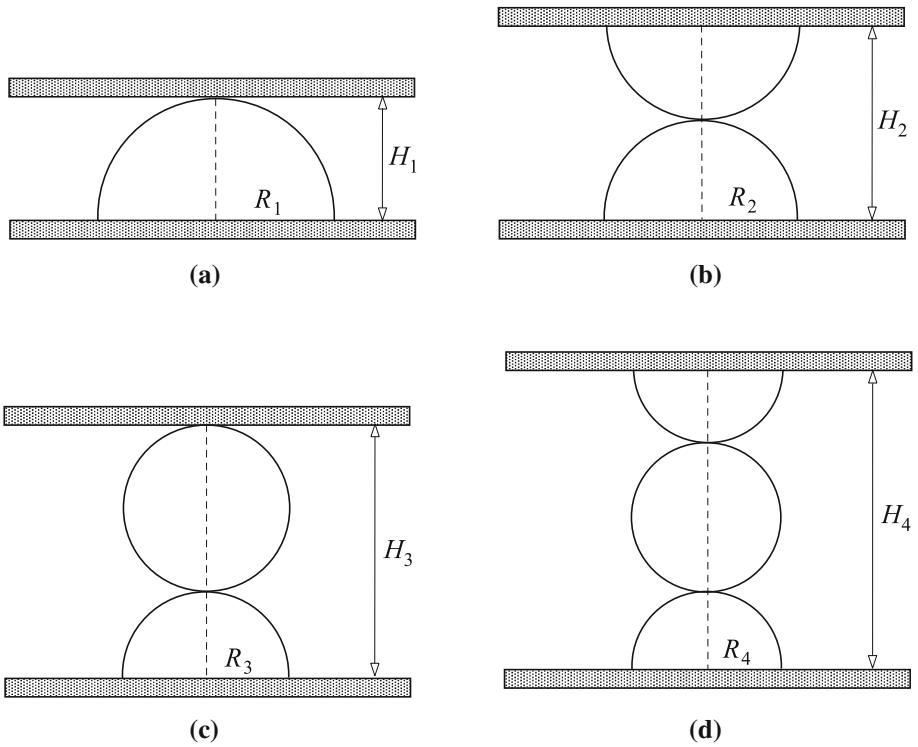

Fig. 3 The equilibrium liquid configurations between two parallel plates consisting of $n \geq 1$ hemispherical drop segments. The liquid volume is the same in all cases, so that the sequence of radii decreases according to $R_n = R_1/n^{1/3}$. The corresponding heights are $H_n = nR_n$

3 Unduloidal equilibrium configurations

In the absence of gravity, the equilibrium shape of the lateral surface of the liquid bridge must be a surface of constant mean curvature (because the pressure difference Δp is constant across such a surface). Since the contact angle with the end plates is 90°, the possible solutions of the capillary equation under zero gravity are circular cylinders and unduloids, with their maximum or minimum radii at the end plates [4,9].[3] The profile of an unduloid segment, sketched in Fig. 4a, is the solution of the nonlinear differential equation $2\sigma\kappa = \Delta p$, where the curvature is defined by the well-known formula

$$2\kappa = \frac{\cos\varphi}{r} - r''\cos^3\varphi, \quad \cos\varphi = \frac{1}{(1+r'^2)^{1/2}}. \tag{9}$$

The first integral of (9) is

$$r\cos\varphi = \kappa r^2 + c. \tag{10}$$

It readily follows from the boundary conditions that the integration constant is $c = \kappa r_a r_b$, while the curvature

$$\kappa = \frac{1}{2r_o} = \frac{1}{r_a + r_b}, \quad r_o = \frac{1}{2}(r_a + r_b), \tag{11}$$

where r_a and r_b are the two base radii. Furthermore, from Eqs. (9) and (11),

$$\frac{2}{r_a + r_b} = \frac{1}{r_a} - r_a'' = \frac{1}{r_b} - r_b'' = \frac{\cos\varphi_*}{r_*}, \tag{12}$$

[3] The profile of an unduloid surface is obtained by tracing the focus of an ellipse as it rolls along a straight line. The unduloid surface is obtained by revolving the so- generated profile (Delaunay arc) around the line of rolling [29,30].

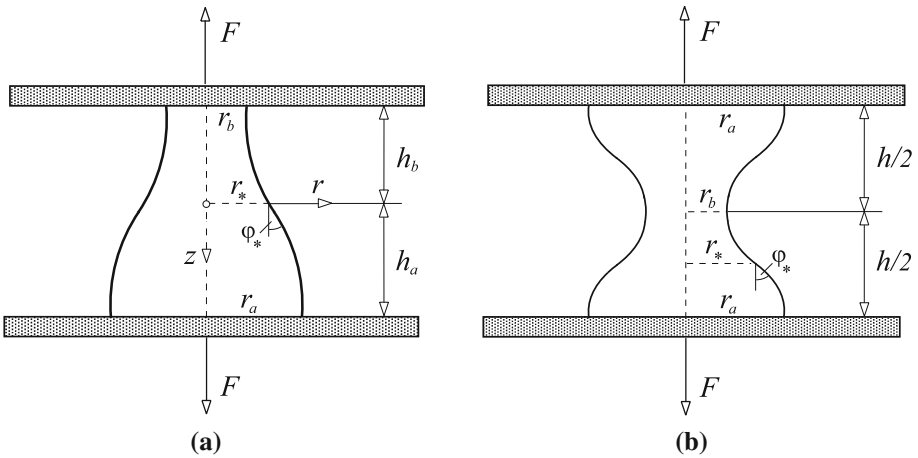

Fig. 4 An unduloidal equilibrium configuration of the liquid bridge with **a** one, and **b** two inflection points

where r_* is the radius at the inflection point, and φ_* is the corresponding slope. Consequently, by exploring (12), we obtain

$$\begin{aligned} &r_*^2 = r_a r_b, \quad \cos\varphi_* = \frac{2r_*}{r_a + r_b}, \quad \sin\varphi_* = \frac{r_a - r_b}{r_a + r_b}, \\ &r_a'' = \frac{r_b - r_a}{r_a(r_a + r_b)}, \quad r_b'' = \frac{r_a - r_b}{r_b(r_a + r_b)}, \quad r_b'' - r_a'' = \frac{r_a - r_b}{r_a r_b}. \end{aligned} \tag{13}$$

Since $\Delta p = \sigma / r_o$, the force required to hold the bridge in equilibrium is

$$F = 2r_*\pi\sigma\cos\varphi_* - r_*^2\pi\,\Delta p = \pi\sigma\,\frac{r_*^2}{r_o} = \pi\sigma r_o\cos^2\varphi_*. \tag{14}$$

The distances from the inflection point to the bottom and top plate are

$$h_{a,b} = r_o[E(k_*) \pm k_*], \quad k_* = \sin\varphi_*, \tag{15}$$

where

$$E(k_*) = \int_0^{\pi/2} (1 - k_*^2\sin^2\theta)^{1/2}\mathrm{d}\theta = \frac{\pi}{2}\left(1 - \frac{1}{4}k_*^2 - \cdots\right) \tag{16}$$

is the complete elliptic integral of the second kind. In particular, $h_a - h_b = r_a - r_b$, so that the profile of the unduloid is not antisymmetric with respect to the inflection point. The total height of the considered unduloidal segment ($h = h_a + h_b$) is

$$h = 2r_o E(k_*) = \pi r_o\left(1 - \frac{1}{4}k_*^2 - \cdots\right). \tag{17}$$

In order that the inflection point is within the height of the bridge, $h_b \geq 0$. If the unduloidal bridge consists of n segments from Fig. 4 so that its profile has n inflection points, the height of the bridge is n times greater than the right-hand side of (17), i.e., $h = 2nr_o E(k_*)$. The unduloidal configuration with two inflection points is sketched in Fig. 4b. Figure 5 shows the variation of the radii r_o, r_*, r_a, and r_b from Fig. 4a versus the increasing height of the unduloid, under constant volume of the enclosed liquid. The scaling length is $\bar{h} = (3V/2\pi)^{1/3}$, which is the radius of a hemispherical drop $R_1 = H_1$ from Fig. 3a. The maximum height in Fig. 5 is $h = h_1 = 1.874H_1$, which corresponds to unduloidal bifurcation to cylindrical shape; see the sequence of heights (27) below. The corresponding variation of the height segments h_a and h_b, whose sum is the total height of the unduloid is shown in Fig. 5b.

The lateral surface and the enclosed volume within the unduloid of Fig. 4a are evaluated in [9]. The expressions are

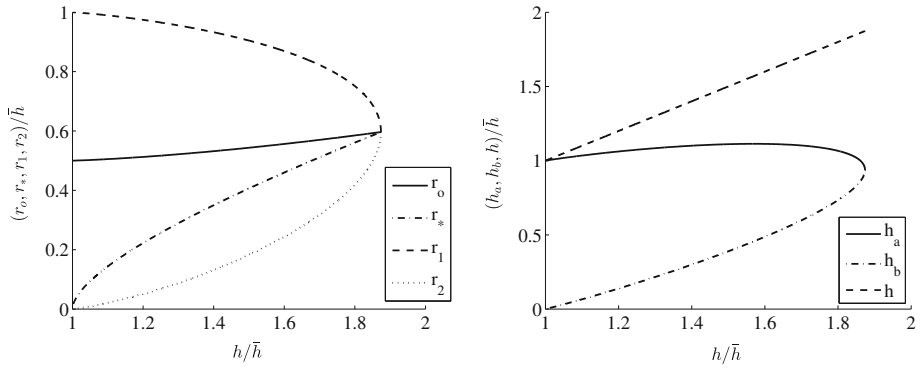

(a) **(b)**

Fig. 5 **a** The variation of the radii r_o, r_*, r_a, and r_b for the unduloidal segment with one inflection point from Fig. 4a versus its height at constant volume. The scaling length is $\bar{h} = R_1 = H_1 = (3V/2\pi)^{1/3}$. **b** The corresponding variation of the height segments h_a and h_b, whose sum is the total height of the unduloid ($h = h_a + h_b$)

$$\begin{aligned} S &= 4\pi r_o^2 \left[2E(k_*) - (1-k_*^2)K(k_*)\right], \\ V &= \frac{2\pi}{3} r_o^3 \left[(7+k_*^2)E(k_*) - 4(1-k_*^2)K(k_*)\right], \end{aligned} \tag{18}$$

where

$$K(k_*) = \int_0^{\pi/2} (1 - k_*^2 \sin^2\theta)^{-1/2} \mathrm{d}\theta = \frac{\pi}{2}\left(1 + \frac{1}{4}k_*^2 + \cdots\right) \tag{19}$$

is the complete elliptic integral of the first kind. To first-order terms in k_*^2, the expressions in (18) simplify to

$$S = 2\pi^2 r_o^2 \left(1 + \frac{1}{4}k_*^2\right), \quad V = \pi^2 r_o^3 \left(1 + \frac{3}{4}k_*^2\right). \tag{20}$$

These can also be expressed, by incorporating the height h, as

$$S = 2\pi r_o h \left(1 + \frac{1}{2}k_*^2\right), \quad V = \pi r_o^2 h \left(1 + k_*^2\right). \tag{21}$$

If the unduloidal bridge configuration consists of n segments shown in Fig. 4a, its surface and volume are n times greater than the right-hand sides of the expressions (18) or (20).

Figure 6a shows the variation of the surface area (S) of the unduloids with one, two, three, or more inflection points versus the height h (normalized by $\bar{S}$ and $\bar{h}$, as indicated). The volume of the liquid is the same for all unduloids. The utilized expressions to construct the plots are

$$\frac{S}{\bar{S}} = 4\pi n^{1/3} \frac{2E(k_*) - (1-k_*^2)K(k_*)}{[(7+k_*^2)E(k_*) - 4(1-k_*^2)K(k_*)]^{2/3}}, \quad \bar{S} = \left(\frac{3V}{2\pi}\right)^{2/3}, \tag{22}$$

$$\frac{h}{\bar{h}} = n^{2/3} \frac{2E(k_*)}{[(7+k_*^2)E(k_*) - 4(1-k_*^2)K(k_*)]^{1/3}}, \quad \bar{h} = \left(\frac{3V}{2\pi}\right)^{1/3} = H_1. \tag{23}$$

They are obtained by combining expressions (17) and (18) and by letting $k_* \in [0, 1]$ to encompass the entire range of unduloidal shapes (from cylindrical to spherical). The unduloids with one inflection point ($n = 1$) are to the left and with more inflection points toward the right. In each range of the height where multiple unduloidal shapes exist, the inequality $S_n > S_{n-1}$ holds. For a given liquid volume and a prescribed lateral surface, either none, one, or two unduloids can fit between two plates. This can be observed from Fig. 6a, because a horizontal line S = const. intersects at most two unduloidal branches. If two unduloidal configurations of the same volume and lateral surface exist (configurations with n and $n+1$ inflection points), the configuration with n inflection points has a greater height.

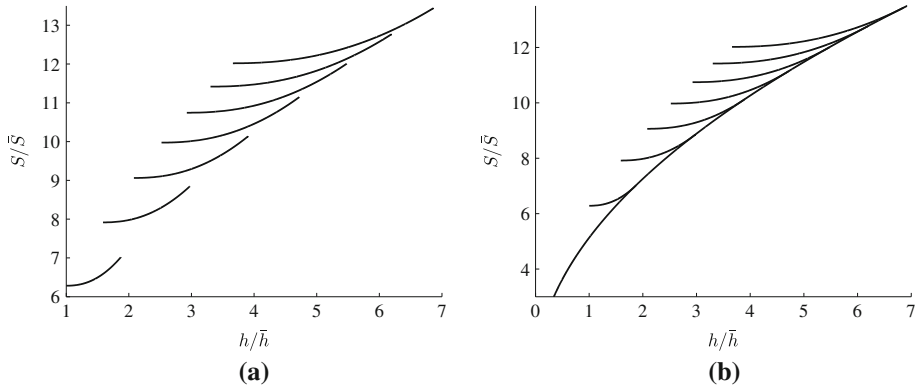

Fig. 6 **a** The variation of the surface area (S) of the unduloids with one, two, three, or more inflection points versus the height h, normalized by $\bar{S}$ and $\bar{h}$, as specified in (22) and (23). The volume of the liquid is the same for all unduloids. **b** The same as in part **a**, with the added parabolic variation of the lateral surface area of the cylindrical bridge. The square root parabola is an envelope of the S-curves for the unduloids corresponding to different n. The bifurcation heights (h_n) are where the S-curves merge into the parabola

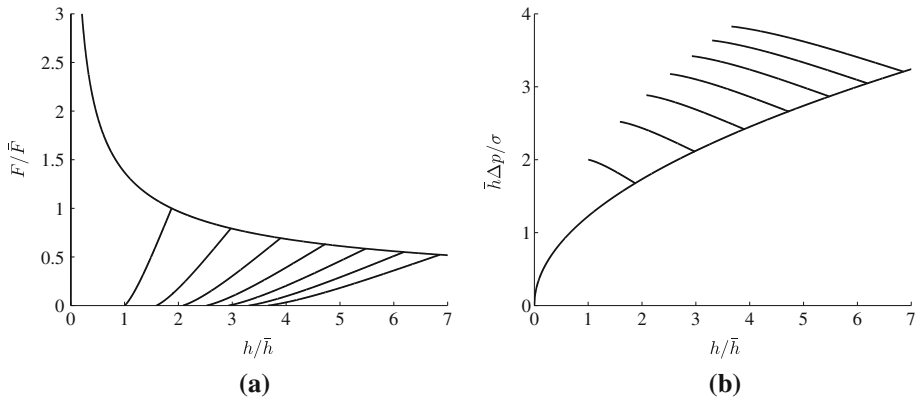

Fig. 7 **a** The variation of the magnitude of the force F required to keep the bridge in equilibrium (scaled by $\bar{F} = (\pi V)^{1/3}\sigma$) versus the height of the bridge. The *curves* corresponding to unduloidal bridge shapes, determined from (24), branch off from the cylindrical bridge curve (29) at the bifurcation heights $h_1, h_2, h_3, \ldots$. The force is equal to zero for the configurations of the type shown in Fig. 3, corresponding to heights $H_1, H_2, H_3, \ldots$. **b** The variation of the capillary pressure Δp (scaled by $\sigma/\bar{h}$) versus the height of the bridge. The *curves* corresponding to the unduloidal bridge shapes are obtained from (30), and for the cylindrical bridge from (31)

The heights corresponding to the end points of each curve S_n in Fig. 6a are specified by the sequence $\{H_n\}$ given by (8). If u_n denotes an unduloid with n inflection points, than for $h < H_1$, the only equilibrium shape is a cylinder (c); for $H_1 < h < H_2$, the possible equilibrium shapes are c and u_1; for $H_2 < h < h_1$, they are c, u_1 and u_2; for $h_1 < h < H_3$, they are c and u_2; for $H_3 < h < H_4$, they are c, u_2 and u_3; and for $H_4 < h < H_5$, they are c, u_2, u_3 and u_4, etc.

The force required to hold the unduloidal bridge in equilibrium is determined from (14) and can be expressed as

$$\frac{F}{\bar{F}} = \left(\frac{3\pi}{2n}\right)^{1/3} \frac{1-k_*^2}{[(7+k_*^2)E(k_*) - 4(1-k_*^2)K(k_*)]^{2/3}}, \quad \bar{F} = (\pi V)^{1/3}\sigma. \tag{24}$$

The variation of this force with the height of the bridge is shown in Fig. 7a.

3.1 Bifurcation from unduloidal to cylindrical shape

The bifurcation of an n-segment unduloidal shape into a cylindrical shape takes place when $k_* \to 0$ in (17) so that the height (h_n) of the so-obtained cylinder is related to the radius of its base (r_n) by $h_n = n\pi r_n$. The

enclosed volume is, from Eq. (20), $V = n\pi^2 r_n^3$. Consequently, the height of the cylindrical bridge can be expressed as

$$h_n = \left(\frac{2\pi^2}{3}\right)^{1/3} H_n \approx 1.8739 H_n, \tag{25}$$

where H_n is defined in terms of the volume V by Eq. (2).

The force required for the equilibrium of this cylindrical bridge is

$$F_n = r_n \pi \sigma = \left(\frac{\pi V}{n}\right)^{1/3} \sigma = \left(\frac{2\pi^2}{3n}\right)^{1/3} H_1 \sigma, \tag{26}$$

which is related to the force $\hat{F}_n$ from Eq. (7) by $\hat{F}_n = (2\pi^2/3)^{1/6} F_n$.

The sequence of the increasing heights $\{h_n\}$, scaled by $\bar{h} = (3V/2\pi)^{1/3}$, for different values of n, is

$$\frac{\{h_n\}}{\bar{h}} = \left(\frac{2\pi^2}{3}\right)^{1/3} \{n^{2/3}\} = \{1.874,\ 2.975,\ 3.898,\ 4.722,\ 5.479,\ 6.187,\ \ldots\}. \tag{27}$$

The two sequences (8) and (27) joined together are

$$\frac{1}{\bar{h}}\{H_1,\ H_2,\ h_1,\ H_3,\ H_4,\ H_5,\ h_2,\ H_6,\ H_7,\ h_3,\ H_8,\ H_9,\ H_{10},\ h_4,\ \ldots\}$$
$$= \{1,\ 1.587,\ \underline{1.874},\ 2.08,\ 2.52,\ 2.924,\ \underline{2.975},\ 3.302,\ 3.659,\ \underline{3.898},\ 4,\ 4.327,\ 4.642,\ \underline{4.722},\ \ldots\}.$$

For convenience, the values corresponding to the members of the bifurcation sequence $\{h_n\}$ are underlined.

Figure 6b shows the same plots as Fig. 6a, with the added parabolic variation of the surface area of the cylindrical bridge versus its height, enclosing the same volume as each unduloid. The governing expression is obtained from $\pi r^2 h = V$ and $S = 2\pi r h$, which gives

$$\frac{S}{\bar{S}} = 2\pi \left(\frac{2h}{3\bar{h}}\right)^{1/2}, \quad \bar{h} = \left(\frac{3V}{2\pi}\right)^{1/3}. \tag{28}$$

This square root-type parabola is an envelope of the family of S-curves for the unduloids with different n. The contact points are the points of the bifurcation from the cylindrical to unduloidal shape, specified by the sequence $\{h_n\}$ from (27). An alternative graphical illustration of the nonuniqueness of equilibrium configurations and the bifurcation points was used in [9], where the plot of the normalized liquid volume versus the normalized capillary pressure was constructed.

The force required to keep the cylindrical bridge in equilibrium is

$$\frac{F}{\bar{F}} = \left(\frac{2\pi^2}{3}\right)^{1/6} \frac{1}{(h/\bar{h})^{1/2}} = \frac{1}{(h/h_1)^{1/2}}, \quad h_1 = \left(\frac{2\pi^2}{3}\right)^{1/3} \bar{h}. \tag{29}$$

This is an envelope of the force-curves for unduloidal bridge shapes, as shown in Fig. 7a. For a given height of the bridge, the force required to keep a cylindrical bridge in equilibrium is greater than the force required for equilibrium of any unduloidal configuration at that height. The force–displacement relation for liquid bridges with arbitrary contact angle is studied in [6].

The capillary pressure within the unduloidal bridge is $\Delta p = \sigma / r_0$, i.e.,

$$\frac{\bar{h}\Delta p}{\sigma} = 2nE(k_*)\left(\frac{h}{\bar{h}}\right)^{-1}, \quad \bar{h} = \left(\frac{3V}{2\pi}\right)^{1/3}. \tag{30}$$

The capillary pressure within a cylindrical bridge is $\Delta p = \sigma / R$, where R is the radius of the base of the cylindrical bridge so that

$$\frac{\bar{h}\Delta p}{\sigma} = \left(\frac{3}{2}\right)^{1/2}\left(\frac{h}{\bar{h}}\right)^{1/2}, \quad \bar{h} = \left(\frac{3V}{2\pi}\right)^{1/3}. \tag{31}$$

The plots are shown in Fig. 7b. For a given height of the bridge, the capillary pressure within a cylindrical bridge is smaller than the capillary pressure within any unduloidal equilibrium configuration at that height. The capillary pressure of latter configurations increases with the increase in the number of their inflection points.

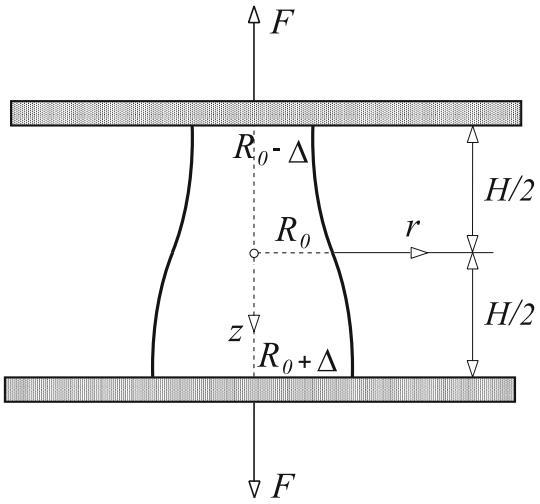

Fig. 8 A sinusoidal perturbation of the cylindrical liquid bridge specified by (32)

4 Stability analysis based on a sinusoidal perturbation

Figure 6 shows that the cylindrical shape of the liquid bridge is energetically preferred over all unduloidal equilibrium shapes (all $n \geq 1$). Nonetheless, the equilibrium configuration of the cylindrical bridge becomes unstable when its height is greater than half of its circumference ($H = \pi R$), as expected from the classical Plateau–Rayleigh instability of a liquid jet, which occurs at $H/R = 2\pi$.[4] This is so because at the onset of instability, there is a nonequilibrium geometrically permissible configuration of the liquid bridge with a lower lateral surface energy. Indeed, assume that the profile of a perturbed shape is of the sinusoidal type (Fig. 8),

$$r = R_0 + \Delta \sin\left(\frac{\pi z}{H}\right). \tag{32}$$

This specifies a surface of revolution which does not have a constant curvature,[5] as required by the Laplace equation $2\sigma\kappa = \Delta p$ (pressure difference being constant in the absence of gravity) so that (32) does not represent a possible equilibrium configuration of the liquid bridge. It is, however, a geometrically (kinematically) admissible configuration for the perturbation analysis, because it satisfies the boundary condition of 90° contact angle with the two end plates. The relationship between R_0 and Δ is specified by the condition that (32) encloses a given volume of the liquid between the plates at a given distance H. This is

$$V = \pi \int_{-H/2}^{H/2} r^2 \, \mathrm{d}z = \pi H \left(R_0^2 + \frac{1}{2}\Delta^2\right). \tag{33}$$

The lateral surface area of the perturbed shape is

$$S = 2\pi R_0 L, \quad L = 2\int_0^{H/2} \left(1 + r'^2\right) \mathrm{d}z, \tag{34}$$

[4] This result is from the static analysis. The kinetic analysis of Rayleigh predicts that the perturbation of wavelength $H \approx 9R$ grows most rapidly [28].

[5] Its curvature, to first-order terms in Δ/H, is

$$\kappa = \frac{1}{2R_0}\left[1 + \left(\pi^2 \frac{R_0}{H} - \frac{H}{R_0}\right)\frac{\Delta}{H} \sin\left(\frac{\pi z}{H}\right)\right],$$

which clearly depends on z.

where L is the length of the perturbed profile curve. By using the approximation $(1+r'^2)^{1/2} \approx 1 + r'^2/2$, it follows that[6]

$$L = H\left(1 + \frac{\pi^2\Delta^2}{4H^2}\right), \quad S = 2\pi R_0 H\left(1 + \frac{\pi^2\Delta^2}{4H^2}\right). \tag{36}$$

If the perturbed shape is energetically preferred over the cylindrical shape, enclosing the same liquid volume, the conditions $S \le 2R\pi H$ and $V = R^2\pi H$ must hold, i.e.,

$$R_0\left(1 + \frac{\pi^2\Delta^2}{4H^2}\right) \le R, \quad R_0^2 + \frac{1}{\Delta^2} = R^2. \tag{37}$$

By squaring both sides of the inequality in (37) and by incorporating the relationship between R_0 , R and Δ, it follows that

$$R_0^2\pi^2 \le H^2 \quad \Rightarrow \quad H \ge \pi R\left(1 - \frac{\Delta^2}{4R^2}\right). \tag{38}$$

This inequality is certainly satisfied, meaning that the considered sinusoidal shape has a smaller surface area than a cylindrical shape, whenever the aspect ratio of the cylinder is $H/R \ge \pi$. Thus, $H/R = \pi$ is the critical aspect ratio for the instability of a cylindrical liquid bridge. In terms of the liquid volume, the height of the cylindrical bridge at the onset of instability is $H = (\pi V)^{1/3}$ so that a cylindrical bridge is unstable if its volume is smaller than H^3/π. From the presented analysis, it also follows that the cylindrical bridge with the volume larger than H^3/π is stable relative to the sinusoidal perturbation (32); Vogel [4] (Theorem 4.3) and Athanassenas [5] (Theorem 3.2) proved its stability for $V > H^3/\pi$ with respect to an arbitrary volume preserving perturbation. Carter [6] performed numerical evaluation of stable bridge configurations for various values of contact angle $\theta \ne 90°$, observing that the volume of every stable liquid bridge was greater than H^3/π. This was known as "Carter conjecture", which was subsequently proved by Finn and Vogel [10]. Zhou [11] extended Finn and Vogel's result and proved that the lower bound for the volume of a stable liquid bridge (H^3/π) also holds when the contact angles with two plates are different. She furthermore improved this lower bound by deriving expressions for higher lower bounds, dependent on whether the profile of stable bridge is a catenoid, a nodoid, or an unduloid with one or no inflection points.

5 Instability of unduloidal equilibrium configurations

It was shown by Vogel [4] that, for an arbitrary but equal contact angle with the end plates, among unduloidal bridge configurations only those with no inflection points between the end plates can be stable, while those with one or more inflection points are always unstable. This means that all unduloidal bridge configurations with 90° contact angle are unstable. We shed in this section additional light to this result, based on the following analysis of the surface energy plots from Fig. 6. For $h < H_1 = (\pi V)^{1/3}$, the cylindrical bridge is the only equilibrium configuration and is stable, as discussed in Sect. 4. For $H_1 < h < H_2$, there are two possible equilibrium configurations, a cylindrical configuration (c) and an unduloidal configuration (u_1) with one inflection point (see Fig. 6b). Since $H_2 < h_1$, and since the cylindrical configuration is stable for $h < h_1$, the unduloidal configuration must be unstable. Indeed, consider the unduloidal configuration u_1 whose height is slightly less than the bifurcation height h_1. If u_1 was stable, all nearby configurations of the same height would have to have a higher energy than u_1; but the plot in Fig. 6 shows that the cylindrical configuration c has smaller energy than u_1. Thus, u_1 must be unstable. Physically, for any u_1, removing a bit of liquid near the bottom of u_1 (where $r_a > r_b$) and adding it near the top (Fig. 4a) would decrease the surface energy of the so-created perturbed configuration. Since u_2, u_3, etc., consist of 2, 3, etc., unstable u_1 segments, all unduloidal bridge configurations are unstable. Their equilibrium configurations are thus associated with the saddle points of the surface energy functional in the space of geometrically admissible surface shapes (Fig. 9b).

[6] The exact evaluation of L actually gives

$$L = \frac{2\Delta}{k}E(k), \quad k^2 = \frac{\pi^2\Delta^2}{H^2 + \pi^2\Delta^2}, \tag{35}$$

where $E(k)$ is the complete elliptic integral of the second kind.

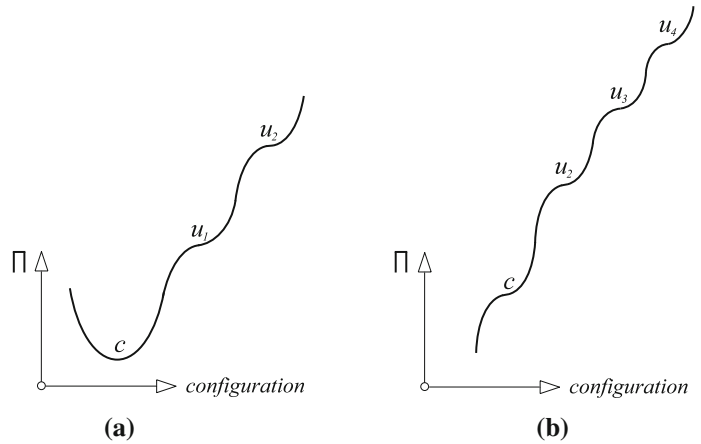

Fig. 9 A schematic representation of the shape of the potential energy $\Pi = \sigma S - (\Delta p)V$ of the liquid bridge whose height h is: **a** $H_2 < h < h_1$, when there are three possible equilibrium configurations (stable cylindrical configuration c, and unstable unduloidal configurations u_1 and u_2), and **b** $H_5 < h < h_2$, when there are four unstable equilibrium configurations (c, u_2, u_3, u_4), all being associated with the saddle points of the potential energy functional

The instability of the unduloidal bridge configuration with one inflection point in the range of height $H_2 < h < h_1$, where there are three possible equilibrium configurations (c, u_1, and u_2, see Fig. 6a) can also be demonstrated by using a sinusoidal perturbation (32). To proceed analytically, since $H_2/h_1 = 1.587/1.874 \approx 0.85$, we adopt the approximate expressions for the surface and volume of the unduloidal shape given by (21). An analogous analysis can be performed numerically by using the exact expressions (18). The surface area and the volume enclosed by the sinusoidal shape (32) are given by (33) and (36). The unduloidal bridge is unstable with respect to this sinusoidal (nonequilibrium) perturbation of the same height $h = H$ and the same volume V, if

$$\pi r_o^2 H \left(1 + k_*^2\right) = \pi H \left(R_0^2 + \frac{1}{2}\Delta^2\right) \tag{39}$$

and

$$2\pi R_0 H \left(1 + \frac{\pi^2 \Delta^2}{4H^2}\right) < 2\pi r_o H \left(1 + \frac{1}{2}k_*^2\right), \tag{40}$$

where the height of the bridge is

$$H = \pi r_o \left(1 - \frac{1}{4}k_*^2\right) < \pi r_o. \tag{41}$$

From (39), it follows that

$$R_0^2 = r_o^2 \left(1 + k_*^2\right) - \frac{1}{2}\Delta^2, \tag{42}$$

while (40) implies $H > R_0\pi$. Thus, in view of (41),

$$\pi R_0 < H < \pi r_o. \tag{43}$$

In order that this inequality holds, the sinusoidal perturbation must be chosen such that $R_0 < r_o$. Since (42) can be rewritten, to first-order terms in k_*^2, as

$$r_o^2 = R_0^2 \left(1 - k_*^2\right) + \frac{1}{2}\Delta^2, \tag{44}$$

we conclude that $R_0 < r_o$ provided that $\Delta > \sqrt{2}R_0 k_*$. It remains to show that $R_0 < R$, because we are considering the height $H < \pi R$, where R is the radius of a cylindrical bridge of the same volume. The inequality $R_0 < R$ is certainly fulfilled, because, from (21), the volume $V = \pi r_o^2 H(1 + k_*^2) = \pi R^2 H$, which

gives $R^2 = r_o^2(1 + k_*^2)$. This proves that $R > r_o$ and thus $R > R_0$, because $R_0 < r_o$ for $\Delta > \sqrt{2}R_0k_*$. Therefore, we have demonstrated that the sinusoidal nonequilibrium perturbation (39) with $\Delta > \sqrt{2}R_0k_*$ has a lower surface energy than the considered unduloidal equilibrium configuration with one inflection point (u_1) so that the latter represents an unstable equilibrium configuration.

6 Lower bound estimates of the critical aspect ratio

Although we presented a static analysis for the determination of the precise value of the critical aspect ratio H/R at which a cylindrical liquid bridge becomes unstable, a simpler analysis can be constructed to obtain a reasonably accurate lower bound estimate of the critical aspect ratio. This analysis is analogous to that from [31] in the case of a liquid jet. If a hemispherical drop configuration is energetically preferred over a cylindrical bridge configuration enclosing the same volume (Fig. 10), its surface energy must be smaller, i.e.,

$$2R_1^2\pi \le 2R\pi H, \quad \frac{2}{3}R_1^3\pi = R^2\pi H \quad \Rightarrow \quad H \ge \frac{9}{4}R = 2.25R. \tag{45}$$

This represents a lower bound estimate of the critical aspect ratio, which implies that instability certainly does not take place for smaller values of the aspect ratio. The predicted critical aspect ratio $H/R = 2.25$ is about 28 % lower than the previously determined static value $H/R = \pi$. In terms of the liquid volume, this simplified analysis predicts that, at the instant of instability, the radius of the cylindrical bridge is $R = (4V/9\pi)^{1/3} = 2R_1/3$ so that the estimated critical height can also be expressed as $H = 3R_1/2$.

Two hemispherical drops are energetically less favored than one hemispherical drop of the same volume, because its total surface area is $\sqrt[3]{4}$ times greater. Consequently, the lower bound of the aspect ratio for the formation of two hemispherical drops (Fig. 11) is twice higher and equal to $H/R = 9/2$. This is again about 28 % lower than the critical aspect ratio $H/R = 2\pi$, corresponding to the transition of the unduloidal bridge with two inflection points into the cylindrical bridge of the same volume. More generally, if the configuration consists of n hemispherical drops of radius R_n, then

$$2nR_n^2\pi \le 2R\pi H, \quad \frac{2n}{3}R_n^3\pi = R^2\pi H \quad \Rightarrow \quad H \ge \frac{9n}{4}R = 2.25nR. \tag{46}$$

The radius of the cylindrical bridge R at the instant of such n-mode instability and the corresponding force are

$$R = \left(\frac{4V}{9n\pi}\right)^{1/3}\sigma, \quad F = \left(\frac{4\pi^2V}{9n}\right)^{1/3}\sigma. \tag{47}$$

The n-mode instability cannot occur below the aspect ratio $H/R = 9n/4$ and above the force $F = (4\pi^2V/9n)^{1/3}\sigma$, which are thus their lower and upper bound estimates, respectively. These expressions

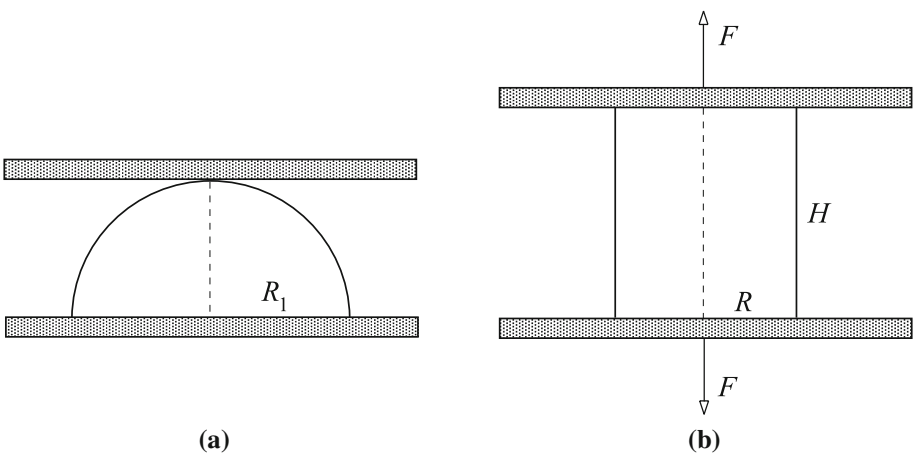

Fig. 10 **a** A hemispherical liquid drop between two parallel plates enclosing the volume $V = 2\pi R_1^3/3$. **b** A cylindrical bridge of the same liquid volume kept in equilibrium by the forces $F = \pi R\sigma$. If two liquid configurations have the same lateral surface, then $R = 2R_1/3$ and $H = 9R/4$

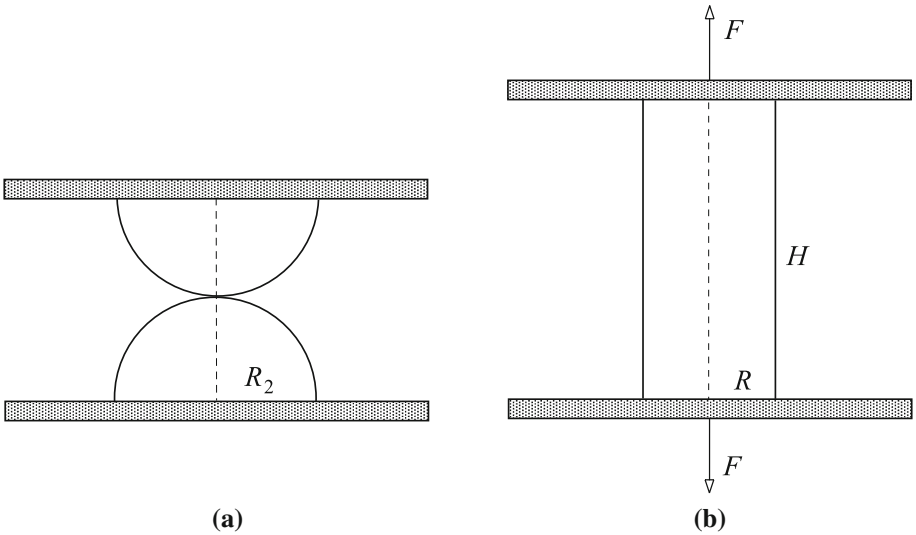

Fig. 11 **a** Two hemispherical liquid drops between two parallel plates enclosing the volume $V = 4\pi R_1^3/3$. **b** A cylindrical bridge of the same liquid volume kept in equilibrium by the forces $F = \pi R\sigma$. If two liquid configurations have the same lateral surface, then $R = 2R_2/3$ and $H = 9R/2$

can be compared with the previously derived expressions for the critical values $H/R = n\pi$, $R = (V/n\pi^2)^{1/3}$, and $F = (V\pi/n)^{1/3}$. While the approximate value of the critical aspect ratio is about 28 % lower, the approximate critical force and the approximate critical radius R are about 12 % higher than their previously determined values. The corresponding height H is about 20 % lower than its true static value.

7 Discussion

We presented a study of the equilibrium and stability of a liquid bridge stretched between two parallel flat plates in the case of 90° contact angle, which is appealing from the physical point of view and its conceptual simplicity. A comprehensive variational analysis was originally presented in [4,5]. The sequence of height intervals is determined for which the unduloidal configurations with different number of inflection points are in equilibrium. The heights at which the bifurcation of a cylindrical bridge shape into an unduloidal shape takes place are also calculated. It is shown that, for a given liquid volume, the lateral surface of a uniform cylindrical bridge is smaller than the surface area of any unduloidal equilibrium shape of the same height. The force required to keep the bridge in equilibrium is evaluated in each case. A simple proof is constructed demonstrating that all unduloidal equilibrium configurations are unstable, confirming the known result that the only stable equilibrium is that of a cylindrical bridge whose height is less than one-half of its circumference. The latter stability is verified relative to a sinusoidal perturbation of the cylindrical shape. A lower bound estimate of the critical aspect ratio is derived by employing a simple energy analysis. The stretching force required to keep the bridge in equilibrium at the onset of instability is compared with its upper bound estimate.

The presented analysis can be extended to more general cases of equal and nonequal contact angles, which are different from 90°. These cases have been studied in the past by many. In the comprehensive analytical and numerical analysis of the stability of liquid bridges by Vogel [7], no stable bridge with an inflection point along its profile was found in the case of arbitrary but equal contact angles at two plates. For contact angles θ less than about 31.1°, he furthermore found that the unduloidal shape of liquid bridge becomes unstable before the appearance of an inflection point, while for θ greater than about 31.1° the stability limit coincides with the appearance of the inflection point (at the end of the bridge, thus with the slope equal to the contact angle). The angle $\theta \approx 31.146°$ was later found to be a unique root of a transcendental equation derived by Langbein [9]. Zhou [12] examined the effect of the contact angle and the liquid volume on the geometry of stable bridge configuration further, specifying when the profile of the bridge is unduloidal, nodoidal, or catenoidal. For example, she found that for the contact angle less than about 15°, the stable bridge configuration is of the nodoidal type (inner portion of it), in agrement with the earlier conclusion from [9]. She also confirmed Vogel's

[7] conclusion that for $\theta > 90°$ all admissible inflectionless convex bridges are stable, while for $\theta < 90°$, not all inflectionless concave bridges are stable, confirming the numerical results from [7–9].

If the contact angles at two plates are different ($\theta_1 \neq \theta_2$), the stability analysis becomes more involved. A stable unduloidal bridge configuration may contain an inflection point between the plates, but no stable bridge with more than one inflection point was detected in numerical experiments by Vogel [7]. See also a related discussion in [13], which also includes the analysis of the gravity effects on the asymmetry of liquid bridge. A slight difference in the wetting properties of the two plates, and thus of their contact angles with the liquid, can have a pronounced effect on the stability of the bridge. Even more striking is an inherent instability associated with a slight tilting of the parallel plates (Concus and Finn [32]). If a bridge between parallel plates is initially not a sphere, it changes discontinuously on an infinitesimal tilt of one of the plates: depending on the contact angles, the bridge either disappears or changes its topology by forming a spherical cap on one of the plates, or an edge blob when the tilted plates touch to form a wedge. A comprehensive analysis of these events can be found in [33].

Acknowledgments Research support from the Montenegrin Academy of Sciences and Arts is gratefully acknowledged. I also express my gratitude to anonymous reviewers for their insightful comments and suggestions.

References

1. Bhushan, B.: Principles and Applications of Tribology. Wiley, New York (1999)
2. Wei, Z., Zhao, Y.-P.: Growth of liquid bridge in AFM. J. Phys. D Appl. Phys. **40**, 4368–4375 (2007)
3. Hotta, K., Takeda, K., Iinoya, K.: The capillary binding force of a liquid bridge. Powder Technol. **10**, 231–242 (1974)
4. Vogel, T.I.: Stability of a liquid drop trapped between two parallel planes. SIAM J. Appl. Math. **47**, 516–525 (1987)
5. Athanassenas, M.: A variational problem for constant mean curvature surfaces with free boundary. J. für Math. **377**, 97–107 (1987)
6. Carter, W.C.: The forces and behavior of fluids constrained by solids. Acta Mettal. **36**, 2283–2292 (1988)
7. Vogel, T.I.: Stability of a liquid drop trapped between two parallel planes II: General contact angles. SIAM J. Appl. Math. **49**, 1009–1028 (1989)
8. Strube, D.: Stability of a spherical and a catenoidal liquid bridge between two parallel plates in the absence of gravity. Microgravit. Sci. Technol. **4**, 104–105 (1991), with the "Correction" in Vol. **5**, 56–57 (1992)
9. Langbein, D.: Stability of liquid bridges between parallel plates. Microgravit. Sci. Technol. **5**, 2–11 (1992)
10. Finn, R., Vogel, T.I.: On the volume infimum for liquid bridges. Z. Anal. Anwendungen **11**, 3–23 (1992)
11. Zhou, L.: On the volume infimum for liquid bridges. Z. Anal. Anwendungen **12**, 629–642 (1993)
12. Zhou, L.: The stability of liquid bridges. Ph.D. Dissertation (available via MathSciNet), Stanford University (1995)
13. Langbein, D.: Capillary surfaces: Shape–Stability–Dynamics, in Particular Under Weightlessness. Springer Tracts in Modern Physics, vol. 178. Springer, Berlin (2002)
14. Slobozhanin, L.A., Alexander, J.I.D., Fedoseyev, A.I.: Shape and stability of doubly connected axisymmetric free surfaces in a cylindrical container. Phys. Fluids **11**, 3668–3677 (1999)
15. Benner, R.E. Jr.., Basaran, O.A., Scriven, L.E.: Equilibria, stability and bifurcations of rotating columns of fluid subjected to planar disturbances. Proc. R. Soc. Lond. A **433**, 81–99 (1991)
16. Kruse, H.P., Mahalov, A., Marsden, J.E.: On the Hamiltonian structure and three-dimensional instabilities of rotating liquid bridges. Fluid Dyn. Res. **24**, 37–59 (1999)
17. Myshkis, A.D., Babskii, V.G., Kopachevskii, N.D., Slobozhanin, L.A., Tyuptsov, A.D.: Low-Gravity Fluid Mechanics. Mathematical Theory of Capillary Phenomena (Springer, Berlin, 1987). [Translated from Russian edition: Gidromekhanika Nevesomosti (Nauka, Moscow, 1976)]
18. Roy, R.V., Schwartz, L.W.: On the stability of liquid ridges. J. Fluid Mech. **391**, 293–318 (1999)
19. Vogel, T.I.: Liquid bridges between balls: the small volume instability. J. Math. Fluid Mech. **15**, 397–413 (2013)
20. Ibrahim, R.A.: Liquid Sloshing Dynamics, Theory and Applications. Cambridge University Press, Cambridge (2005)
21. Meseguer, J., Espino, J.L., Perales, J.M., LLaverón-Simavilla, A.: On the breaking of long, axisymmetric liquid bridges between unequal supporting disks at minimum volume stability limit. Eur. J. Mech. B **22**, 355–368 (2003)
22. Prange, M., Wanschura, M., Kuhlmann, H.C., Rath, H.J.: Linear stability of thermocapillary convection in cylindrical liquid bridges under axial magnetic field. J. Fluid Mech. **394**, 281–302 (1999)
23. Padday, J.F.: Capillary in microgravity. In: Pétré, G. Sanfeld, A. (eds.) Capillarity Today. Lecture Notes in Physics, vol. 386. Springer, New York, pp. 90–107 (1991)
24. Blokhuis, E.M.: Liquid drops at surfaces. In: Hartland, S. (ed.) Surface and Interfacial Tension: Measurement, Theory, and Applications, Surfactant Science Series, vol. 119, pp. 174–193. Marcel Dekker Inc., New York (2005)
25. Lubarda, V.A., Talke, K.A.: Analysis of the equilibrium droplet shape based on an ellipsoidal droplet model. Langmuir **27**, 10705–10713 (2011)
26. Lubarda, V.A.: Mechanics of a liquid drop deposited on a solid substrate. Soft Matter **8**, 10288–10297 (2012)
27. Lubarda, V.A.: The shape of liquid surface in a uniformly rotating cylinder in the presence of surface tension. Acta Mech. **224**, 1365–1382 (2013)
28. Gennes, P.G.de , Brochard-Wyart, F., Quéré, D.: Capillarity and Wetting Phenomena. Springer, Berlin (2004)
29. Finn, R.: Equilibrium Capillary Surfaces. Springer, New York (1986)
30. Kenmotsu, K.: Surfaces with Constant Mean Curvature. American Mathematical Society, Providence, RI (2003)

31. Srolovitz, D.J., Safran S., A.: Capillary instabilities in thin films. J. Appl. Phys. **60**, 247–260 (1986)
32. Concus, P., Finn, R.: Discontinuous behavior of liquids between parallel and tilted plates. Phys. Fluids **10**, 39–43 (1998)
33. Concus, P., Finn, R., McCuan, J.: Liquid bridges, edge blobs, and Sherk-type capillary surfaces. Indiana Univ. Math. J. **50**, 411–441 (2001)